Preprint
UCRL-JC-138104

Defect Diffusion during Annealing of Low-Energy Ion-Implanted Silicon

P.J. Bedrossian, M.-J. Caturla, T. Diaz de la Rubia

This article was submitted to Materials Research Society Conference " Microstructure Evolution during Irradiation, Boston, MA, December 2-5, 1996

March 8, 2001

U.S. Department of Energy

Lawrence
Livermore
National
Laboratory

DISCLAIMER

DEFECT DIFFUSION DURING ANNEALING OF LOW-ENERGY ION-IMPLANTED SILICON

P. J. BEDROSSIAN *, M.-J. CATURLA, AND T. DIAZ DE LA RUBIA
Lawrence Livermore National Laboratory, Livermore CA 94551
*bedrossian1@LLNL.gov

ABSTRACT

We present a new approach for investigating the kinetics of defect migration during annealing of low-energy, ion-implanted silicon, employing a combination of computer simulations and atomic-resolution tunneling microscopy. Using atomically-clean Si(111)-7x7 as a sink for bulk point defects created by 5 keV Xe and Ar irradiation, we observe distinct, temperature-dependent surface arrival rates for vacancies and interstitials. A combination of simulation tools provides a detailed description of the processes that underly the observed temperature-dependence of defect segregation, and the predictions of the simulations agree closely with the experimental observations.

INTRODUCTION

The kinetics of point defects in silicon have generated controversy for many years [1,2,3,4]. In particular, while recent Molecular Dynamics (MD) simulations indicate lower binding energies for vacancy clusters than for interstitials [5], supporting experimental data are scarce. The current, poor state understanding of these properties of defects in silicon poses both a challenge for fundamental semiconductor physics and a formidable obstacle for the development of predictive models of silicon bulk processing.

We investigate the relative stabilities of point defect clusters in Si with a new experimental approach using atomically-clean Si(111) surfaces as a sinks for vacancies and interstitials, coupled with simulations bridging multiple time scales. The arrival of a vacancy (interstitial) at an atomically-clean and flat surface would cause the disappearance (reappearance) of a surface atom. We measure net arrival rates of vacancies and interstitials directly, using the STM to count the number of atoms populating the surface layer after various stages of annealing at different temperatures. We find that after room-temperature irradiation of Si(111)-7x7 by 5keV Ar or Xe ions at submonolayer doses, annealing at 350°C results in a decrease in the atomic population of the adatom layer, while subsequent annealing at 500°C restores the population of that layer.

Modeling of the formation and evolution of defects and defect clusters requires accurate representation and linking of two distinct time scales: (i) the initial cascade, creation, recombination, and clustering of point defects, culminating in the primary damage state (picoseconds), and (ii) the subsequent evolution of the damage under annealing, at experimentally-accessible time scales (seconds and hours.) MD simulations provide a three-dimensional representation of the location of all the defects induced by the implantation process and provide input to the Kinetic Monte Carlo (KMC) simulations, which describe defect evolution over time scales comparable to the experiments. Application of combined MD and KMC simulations shows that the experimental results can be explained by different rates of arrival to the surface of the vacancies and interstitials produced in the bulk during ion irradiation.

EXPERIMENT

The experiments were performed in an ultrahigh vacuum (UHV) system with base pressure below 10^{-10} torr. Si(111) samples cut from commercial wafers exhibited the

7×7 reconstruction in both Low Energy Electron Diffraction (LEED) and STM after annealing at 1250°C for 30 seconds and cooling to room temperature. The STM reveals that step bunching results in typical terrace lengths exceeding 1μm, with occupation of over 99.7% of the atomic sites in the adatom layer, the outermost atomic layer and that which is imaged with the STM. Such surfaces were then exposed briefly to irradiation by 5keV Xe ions, with a total dose of ~1.5×10^{13} cm^{-2}, and imaged *in situ* by STM. After subsequent annealing cycles, the sample was always allowed to cool to room temperature before imaging. Sample temperatures during annealing were recorded with a pyrometer which was calibrated with a thermocouple, and are expected to be accurate within 20°C.

RESULTS

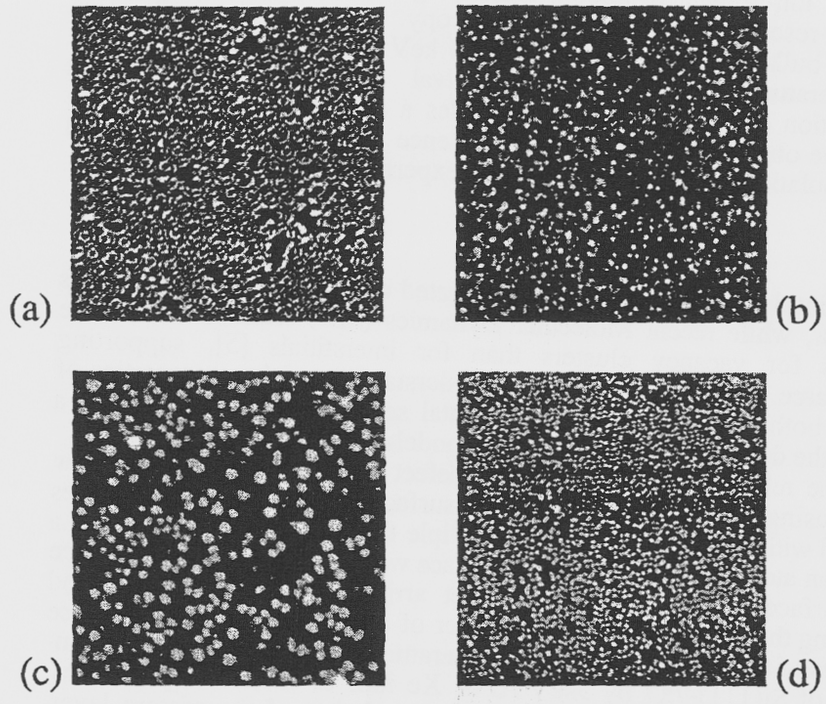

Figure 1: 400Å STM images of the adatom layer of Si(111)-7x7 (a) after initial, room-temperature irradiation by 5 keV Xe ions, at 1.5×10^{13} cm^{-2}, (b) after annealing at 350°C for 5 minutes and (c) after 4 hours, and (d) after annealing at 500°C for 2 minutes.

Figure 1(a) shows a 400Å STM image of Si(111)-7x7 immediately following irradiation by 5keV Xe ions. While the irradiation has resulted in the disappearance of 8% of the atoms from the adatom layer, the long-range surface order is still present in both STM and LEED. Figures 1(b-d) display STM images following progressive stages of annealing of the surface irradiated with Xe ions. While we cannot image exactly the same location after each annealing cycle, we believe on the basis of measurements at various positions on the surface that regions which are imaged generally represent the morphological characteristics of the sample. Annealing at 350°C leads to disappearance of the adatoms from the surface. While those remaining still assume binding sites consistent with the (7x7) superlattice, the percentage of sites occupied drops from 92%

immediately after irradiation to 35% after 5 minutes of annealing (fig. 1(b)), and to 28% after 4 hours of annealing (fig. 1(c)). Despite this depopulation of the adatom layer, the persistence of strong 7x7 periodicity in LEED indicates preservation of the crystalline order in the layers immediately below the adatom layer. Annealing smooth Si(111)-7x7 which has not been exposed to ion irradiation does not lead to adatom disappearance.

Annealing the same surface at 500°C for 2 minutes results in repopulation of 73% of the adatom layer, as in figure 1(d). The strong coherence of the reconstruction demonstrates that it was not disrupted by either the irradiation or the subsequent 350°C anneal. The observed saturation of the adatom layer's population around 75% at 500°C suggests that the repopulation does not result from adatom detachment at steps. We find neither adatom islands nor single-atomic height terraces at the base of step bunches.

Atomistic simulation of both ion implantation and the evolution of induced damage is consistent with a model in which the surface acts as a sink for bulk vacancies and interstitials. Classical MD simulations, with the Stillinger-Weber potential [6] for Si and a Universal pair potential [7] for Si-Xe, in computational boxes with up to 10^6 atoms, are used to model the prompt (10^{-11} s) displacement cascade process that gives rise to the primary state of damage. [8] The concentration of disorder in amorphous pockets and average sputter yield of 2.25 atoms/ion are consistent with previous reports [9, 10].

The dose of $1.5x10^{13}$ ions/cm^2 is accumulated by incorporating 152 ion trajectories in a 0.32x0.32x5 μm box which is used for KMC simulations. Defects produced by the implantation evolve during annealing through point defect diffusion, clustering and cluster evaporation [11], according to recently-calculated diffusivities for vacancies and interstitials in Table I [5, 12]. The prefactor for the self interstitial diffusivity has been obtained by fitting KMC results to the diffusion of boron in silicon [12] and using *ab initio* results for the energetics of the boron-silicon interaction [13]. Binding energies of larger clusters are fitted to the functional form: $Eb_V(n) = 3.6 - 4.9(n^{2/3}-(n-1)^{2/3})$ eV and $Eb_I(n)=2.5-2.17(n^{1/2}-(n-1)^{1/2})$ eV, for V and I clusters of size n, respectively [11].

		Binding Energies of Clusters			
	Diffusivity (cm^2/s)	Size 2 (eV)	Size 3 (eV)	Size 4 (eV)	Size 5 (eV)
Vacancy	0.001exp(-0.43/KT)	0.62	0.78	1.2	1.82
Interstitial	5exp(-0.9/KT)	1.6	2.25	1.29	2.29

Table I. Kinetic parameters in KMC calculations, obtained from MD simulations using the Stillinger-Weber potential [5]. The pre-factor for Interstitial diffusivity was obtained by fitting KMC results to boron diffusion in silicon [12].

We first examine evolution of the damage produced by 5 keV Xe during annealing at 350°C. The KMC simulation first recombines all Frenkel (V-I) pairs within 1 nearest-neighbor. Defects then migrate according to the rules in Table 1. According to the simulations, at 350°C vacancies initially arrive at the surface at a greater rate than do interstitials. The number of vacancies reaching the surface after 4 hours' annealing at 350°C is greater than the number of interstitials. The surface vacancy density is then $0.8x10^{14}$ /cm^2, in reasonable agreement with the experimental observation of $1.2x10^{14}$/cm^2, which in turn represents more than 6 excess vacancies per ion reaching

the surface and greatly exceeds the sputter yield. We note that the total number of vacancies in the adatom layer is not a measure of the sputter yield.

The evolution of defects in the bulk proceeds in two stages: first, when both free vacancies and interstitials are present, the process is governed by the different mobilities of the defects. At 350°C, the diffusivities of V and I are similar, and both diffuse and recombine in the bulk or at the surface. After 10^{-7} s only defect clusters remain in the bulk. In the second stage, corresponding to experimentally measurable times, defect evolution is governed by cluster binding energies. Interstitial clusters dissociate at a much lower rate than vacancies.

After annealing for four hours, 42% of the defects created initially have recombined in the bulk, leaving only 5 V/ion and 9 I/ion in clusters. Increasing the temperature to 500°C induces dissociation of both vacancy and interstitial clusters. According to the simulations, all vacancies quickly disappear from the bulk, leaving only interstitial clusters, whose gradual dissolution releases interstitials which migrate to the surface and cause the observed recovery of the adatom layer. The simulations' predictions of the net numbers of defects appearing on the surface after various annealing times are compared with the experimental results in Table II.

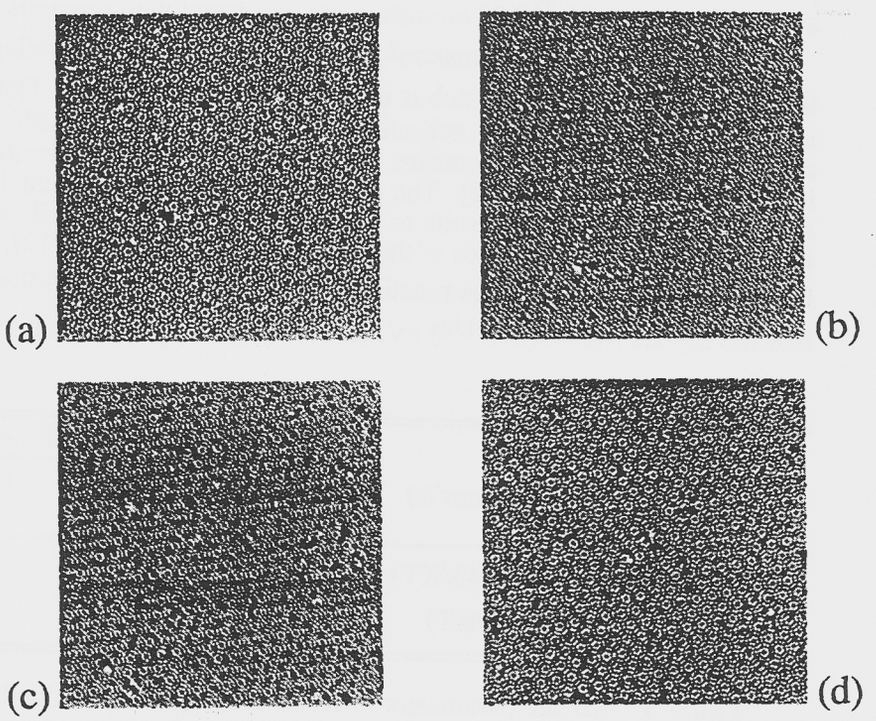

Figure 2: 500Å STM images of Si(111)-7x7 (a) following initial, room-temperature irradiation by 5 keV Ar ions, at 3.5×10^{12} cm^{-2}, (b) after annealing at 350°C for 90 seconds and (c) after 4 minutes, and (d) after annealing at 500°C for 4 minutes.

In order to ensure that the essential result does not arise from a unique combination of ion energy and mass, a similar experiment was performed with a 5 keV Ar ions instead of Xe, and with a lower total dose of 3.5×10^{12} ions/cm^2. Figure 2(a) shows a 500Å STM image of a Si(111)-7x7 surface immediately following the room-temperature Ar irradiation. In this case, 2.4% of the atoms in the adatom layer were missing after the

irradiation. The number increased to 6.4% after 90 sec at 350°C (figure 2(b)), and to 6.8% after 4 minutes at 350°C (figure 2(c)), but dropped to 4.3% after 4 minutes at 500°C. Corresponding, combined MC and KMC simulations for 5 keV Ar impacts on Si(111) and subsequent annealing also predict a net surface segregation of vacancies at 350°C, and a net arrival of interstitials at 500°C after the vacancy clusters have dissolved. The simulations' predictions of the net numbers of defects appearing on the surface after various annealing times are compared with the experimental results for this case in Table II below.

Room-Temp. Irradiation	Annealing Temp. (°C)	Annealing Time	Surface Defects/cm^2 Experiment	Simulation
5 keV Xe 1.7×10^{13}/cm^2	350	300	1.2×10^{14} V	1.0×10^{14} V
	350	14400	1.3×10^{14} V	1.0×10^{14} V
	500	240	0.9×10^{14} I	1.0×10^{14} V
5 keV Ar 3.5×10^{12}/cm^2	350	90	1.2×10^{13} V	1.1×10^{13} V
	350	600	1.3×10^{13} V	1.1×10^{13} V
	500	240	4.5×10^{12} I	2.0×10^{12} I

Table II: Comparison of experimentally observed surface defect densities for each of the conditions of irradiation and subsequent annealing described in the text, with defect densities predicted by the simulations. V = "Vacancies," and I = "Interstitials."

CONCLUSIONS

The observed depopulation of the Si (111)-7x7 adatom layer under annealing at 350°C following initial, room-temperature ion irradiation indicates a net surface accumulation of bulk vacancies created by the irradiation and results from the lower binding energy of vacancy clusters than for interstitial clusters. The repopulation of the adatom layer observed upon subsequent annealing at 500°C indicates a net arrival of bulk intersitials which gradually evaporate from the remaining clusters in the bulk after the less stable vacancy clusters have evaporated.

Annealing of damage induced by low-energy implantation in Si leads to the formation of vacancy and interstitial clusters within $\approx 1\mu s$. The kinetics of subsequent damage evolution are controlled by the relative stabilities of interstitial and vacancy clusters. Vacancy clusters, being less stable than interstitial clusters, dissolve at lower temperatures.

ACKNOWLEDGMENTS

The authors are grateful to M. Jaraiz and G. Gilmer of Lucent Technologies for KMC code, and to L. Pelaz for helpful discussions.

This work was performed under the auspices of the U.S. Department of Energy by the University of California, Lawrence Livermore National Laboratory under Contract No. W-7405-Eng-48.

REFERENCES

1. J.D. Plummer, P.G. Griffin, Nucl. Instrum. Meth. **B102,** 160 (95).

2. U. Gösele and T.Y. Tan Diffusion in Solids, Unsolved Problems (Trans Tech. Publications, Zurich, 1992), p.189.

3. H.-J. Gossmann, P.A. Stolk, D.J. Eaglesham, G.H. Gilmer, and J.M. Poate, Process Physics and Modeling in Semiconductor Technology, editied by G.R. Srinivasan, C.S. Murthy, and S.T. Dunham (Electrochemical Society, Pennington, New Jersery, 1996).

4. U. Gösele, A. Plößl, and T.Y. Tan Process Physics and Modeling in Semiconductor Technology, edited by G.R. Srinivasan, C.S. Murthy and S.T. Dunham (Electrochemical Society, Pennington, New Jersey, 1996), p. 309.

5. G.H. Gilmer, T. Diaz de la Rubia, D. Stock and M. Jaraiz, Nucl. Instrum. and Methods **B102,** 247 (1995).

6. F.H. Stillinger and T.A. Weber, Phys. Rev. **B31,** 5262 (1985).

7. J.P. Biersack and J.F. Ziegler, Nucl. Instrum. and Methods. **194,** 93 (1982).

8. M. J. Caturla, L. Marques, T. Diaz de la Rubia and G.H. Gilmer, Phys. Rev. B (in press).

9. J. Narayan, O.S. Oen, D. Fathy and O.W. Hollan, Materials Letters **3,** 67 (1985).

10. P.C. Zalm, J.Appl. Phys. **54,** 2660 (1983).

11. M. Jaraiz, G.H. Gilmer, J. M. Poate and T. Diaz de la Rubia, Appl. Phys. Lett. **68,** 409 (1996).

12. L. Pelaz and G.H. Gilmer (private communication).

13. J. Zhu, T. Diaz de la Rubia, L. Yang, C. Mailhiot and G.H. Gilmer, Phys. Rev. **B54,** 4741 (1996).